4.6 NEUTRON IRRADIATION EFFECTS IN TUNGSTEN — L.M. Garrison, P. Edmondson, N.A.P. Kiran Kumar, T. Colling, M. McAlister, L. Snead, T. S. Byun, D. Lewis (Oak Ridge National Laboratory), and M. Fukuda (Tohoku University, Japan)

OBJECTIVE

The objective of this work is to evaluate the effects of neutron irradiation on the mechanical properties and microstructure of tungsten-based materials to aid in developing plasma-facing materials for fusion reactors.

SUMMARY

A total of 440 samples were irradiated in HFIR at temperatures from 70 to 900°C and fast neutron fluences of 0.01 to 20 $\times 10^{25}$ n/m^2 at E>0.1 MeV. Types of tungsten irradiated in this study were [110] single crystal tungsten, [100] single crystal tungsten, wrought tungsten foils, annealed tungsten foils, and tungsten-copper laminates. Analysis of room temperature tensile test data of the single crystal samples reveals that ultimate strength decreases at less than 1 dpa. The copper tungsten laminate tensile tests were completed and fracture analysis is underway. Atom probe analysis of a single crystal tungsten sample irradiated to 2.2 dpa at approximately 750°C revealed rod-like, ribbon-like, and clusters-shaped Os and Re rich precipitates. Tungsten foils irradiated to 2.2 and 3.8 dpa are being prepared for TEM analysis.

PROGRESS AND STATUS

Mechanical Properties

The hardness data previously reported was re-analyzed by grouping the samples based on their irradiation temperature (Figure 1). For these tungsten samples, the conversion 1×10^{25} n/m^2 (E>0.1 MeV) ≈ 0.32 dpa was used. For both the [100] and [110] samples, the hardness increases with increasing dose, but there is no clear trend with increasing irradiation temperature.

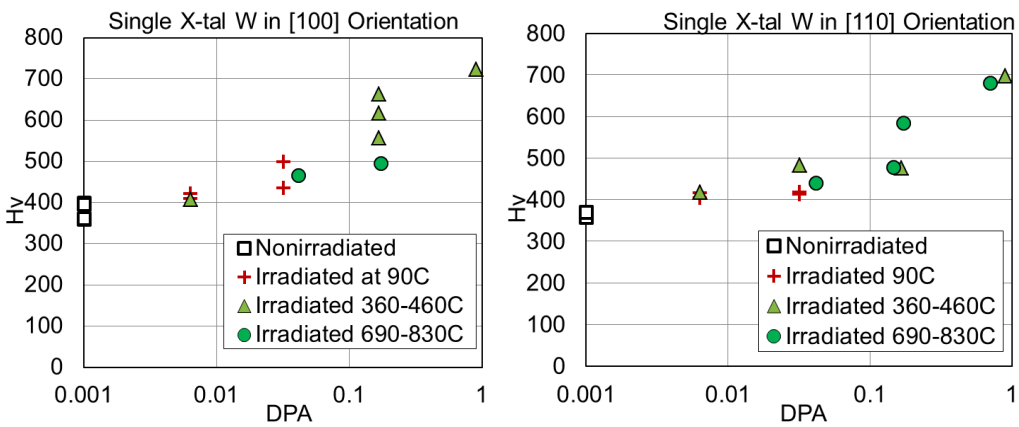

Figure 1. Hardness (Hv) of single crystal tungsten irradiated up to 1 dpa.

Strain gauges were not used during the tensile tests, so the crosshead motion was used to estimate the deformation of the samples. The x-axis for the tensile data is elongation calculated as

$$\text{(crosshead displacement)/(original gauge length)*100\%} \quad (1)$$

Both the [100] and [110] orientation unirradiated tensile samples exhibited non-zero ductility starting at 300°C test temperature (Figure 2Figure 3). For the [110] sample unirradiated and tested at room temperature, the fracture occurred alomg a diagonal across the gauge section with little to no deformation

near the fracture surface (Figure 2a). At the highest test temperature of 650°C there is significant deformation and elongation in the gauge section (Figure 2b). The deformation occurred along the same diagonal as the fracture at room temperature.

For the [100] unirradiated samples, the room temperature fracture occurred perpendicular to the [100] axis of the tensile bar (Figure 3a). Starting at 300°C the [100] samples experienced ductile fracture. The sample tested at the highest temperature of 650°C had significant elongation (Figure 3b).

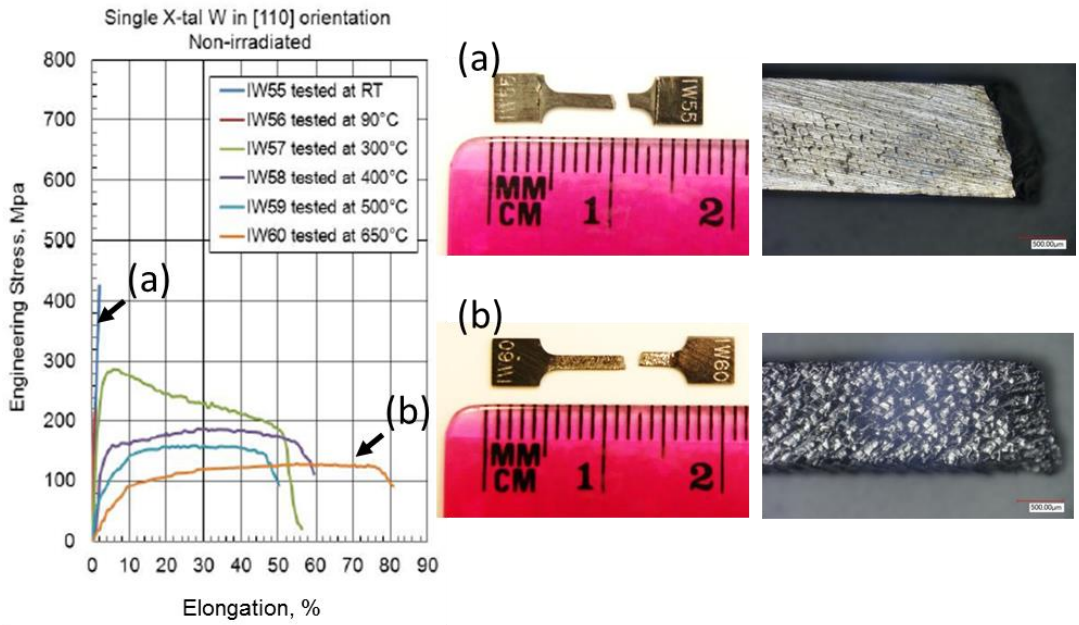

Figure 2. Unirradiated [110] tungsten tensile tested from room temperature to 650°C. (a) no significant deformation is observed on the sample tested at room temperature. (b) the sample tested at 650°C shows significant deformation before fracture.

After irradiation to 0.03 dpa at 90°C, both the [100] and [110] samples still exhibited tensile ductility starting at 300°C test temperature. However, the elongation of the [110] sample tested at 300°C is significantly greater than the [100] sample at the same conditions.

The ultimate tensile strengths of single crystal tungsten samples irradiated at higher temperatures and tensile tested at room temperature are plotted in Figure 5. The fracture behavior of all of these samples was brittle with no plastic deformation observed. At low dpa, the ultimate strength increases as compared to the unirradiated sample strengths. However, as the dpa increases further, starting near ~0.1 dpa, the ultimate strengths decreased.

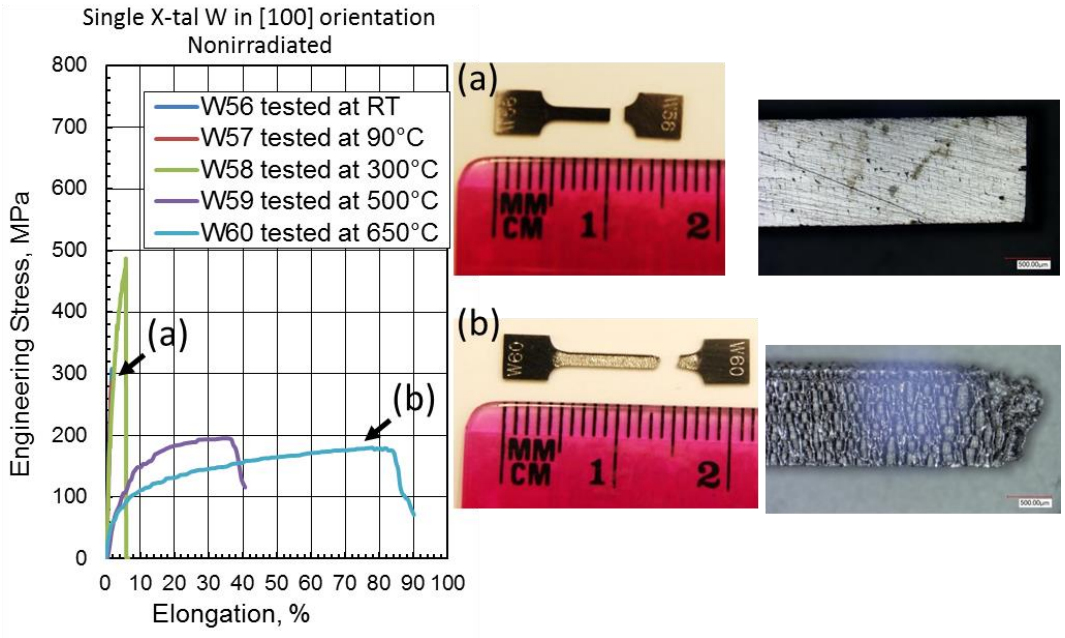

Figure 3. Unirradiated [100] tungsten tensile tested from room temperature to 650°C. (a) no significant deformation is observed on the sample tested at room temperature and the fracture is perpendicular to the tensile axis. (b) the sample tested at 650°C shows significant deformation before fracture.

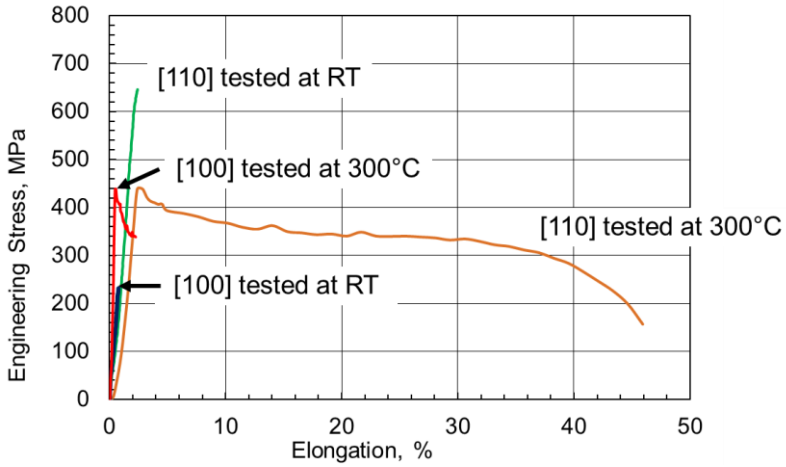

Figure 4. Single crystal tungsten tensile behavior for material irradiated to 0.03 dpa at 90°C.

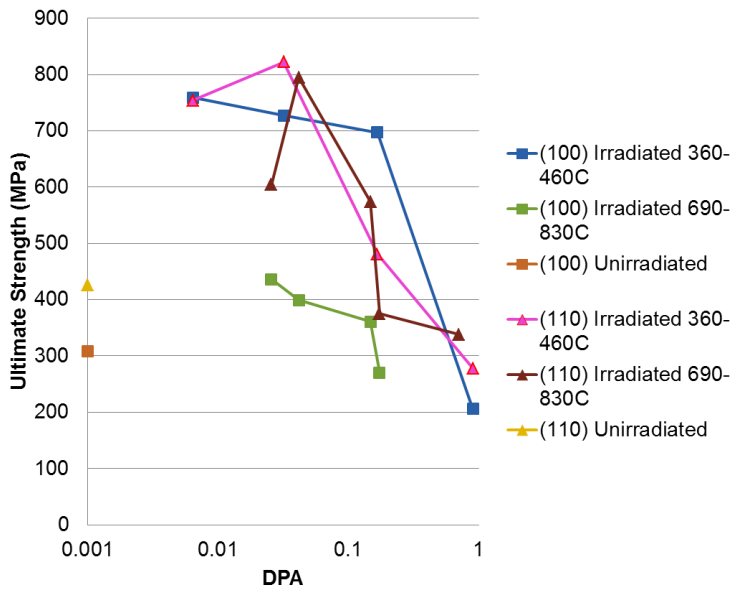

Figure 5. Room temperature ultimate tensile strength of irradiated single crystal tungsten.

Copper-Tungsten Laminates

Tensile tests have been conducted on the copper-tungsten laminate composites. To remove artifacts in the data from the machine compliance, the elastic section of each curve was removed to isolate the plastic deformation section, as in the example in Figure 6. Then, each of the resulting tensile curves was analyzed and evaluated for yield strength, ultimate tensile strength, ultimate elongation, and total elongation (Table 1. **Tensile properties of Cu-W laminate composites.**).

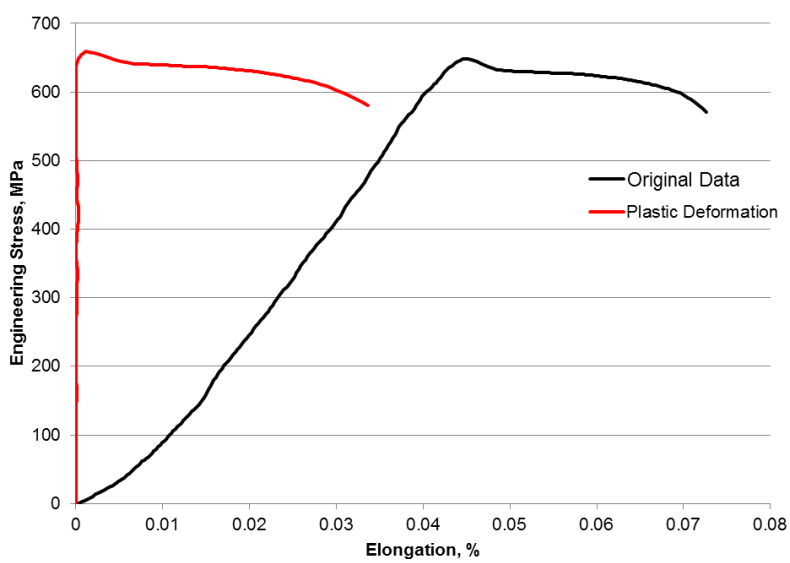

Figure 6. Engineering stress vs. elongation of unirradiated Cu-W laminate composite sample SW36 tested at 650°C.

Table 1. Tensile properties of Cu-W laminate composites.

Specimen Identification	*HFIR Rabbit Capsule*	*Irradiation Temp. (°C)*	*Fast Fluence 10^{25}n/m^2 (E>0.1 MeV)*	*Test Temp (°C)*	*Yield Stress (MPa)*	*Ultimate Tensile Stress (MPa)*	*Uniform Elon-gation (%)*	*Total Elon-gation (%)*
SW40	*unirradiated*	*unirradiated*	*unirradiated*	*22*	*896*	*916*	*0.75*	*15.5*
SW06	*TB-300-1*	*414*	*0.02*	*22*	*1128*	*1131*	*0.22*	*3.7*
SW05	*TB-300-1*	*414*	*0.02*	*22*	*1054*	*1073*	*0.42*	*7.5*
SW07	*TB-300-2*	*448*	*0.1*	*22*	*Brittle Fracture*	*728*	*0*	*0.05*
SW17	*TB-300-3*	*420*	*0.52*	*22*	*1134*	*1139*	*0.09*	*1.4*
SW01	*T9G-11*	*452*	*2.82*	*22*	*Brittle Fracture*	*366*	*0*	*0.01*
SW40	*unirradiated*	*unirradiated*	*unirradiated*	*22*	*896*	*916*	*0.75*	*15.5*
SW12	*TB-500-1*	*751*	*0.08*	*22*	*Brittle Fracture*	*622*	*0*	*0.02*
SW13	*TB-500-2*	*667*	*0.54*	*22*	*Brittle Fracture*	*1033*	*0.08*	*0.08*
SW16	*T9C-14*	*706*	*2.2*	*22*	*Brittle Fracture*	*1245*	*0*	*0.03*
SW15	*T9C-14*	*706*	*2.2*	*22*	*Brittle Fracture*	*1104*	*0*	*0.04*
SW19	*TB-500-3*	*633*	*9*	*22*	*Brittle Fracture*	*691*	*0.1*	*0.15*
SW40	*unirradiated*	*unirradiated*	*unirradiated*	*22*	*896*	*916*	*0.75*	*15.5*
SW23	*TB-650-1*	*776*	*0.13*	*22*	*1141*	*1141*	*0.2*	*1.04*
SW25	*TB-650-2*	*759*	*0.46*	*22*	*Brittle Fracture*	*1244*	*0.15*	*0.15*
SW39	*unirradiated*	*unirradiated*	*unirradiated*	*300*	*457*	*575*	*3.93*	*16.7*
SW38	*unirradiated*	*unirradiated*	*unirradiated*	*400*	*434*	*548*	*4.18*	*12.2*
SW37	*unirradiated*	*unirradiated*	*unirradiated*	*500*	*358*	*448*	*2.15*	*9.8*
SW36	*unirradiated*	*unirradiated*	*unirradiated*	*650*	*318*	*408*	*3.04*	*7.8*
SW08	*TB-300-2*	*448*	*0.1*	*300*	*733*	*741*	*0.41*	*9*
SW18	*TB-300-3*	*420*	*0.52*	*300*	*909*	*909*	*0.2*	*1.3*
SW11	*TB-500-1*	*751*	*0.08*	*750*	*479*	*484*	*0.47*	*4.9*
SW14	*TB-500-2*	*667*	*0.54*	*670*	*Brittle Fracture*	*703*	*0.17*	*0.17*
SW24	*TB-650-1*	*776*	*0.13*	*780*	*496*	*522*	*0.56*	*3.9*
SW26	*TB-650-2*	*759*	*0.46*	*650*	*659*	*661*	*0.17*	*3.4*

SEM and optical microscope images are being taken of the samples, starting with the unirradiated, control samples. Unirradiated laminate sample SW36 tested at 650°C (Figure 7) did not develop any of the surface features in the gauge section that the unirradiated single crystal tungsten samples did when tested at the same temperature (Figure 2Figure 3). From the top view in Figure 7 the pull out of the copper layer is just visible on the right half of the sample.

Figure 7. Optical image of unirradiated Cu-W laminate sample SW36 tensile tested at 650°C.

The optical image of the fracture surface of SW36 (Figure 8), shows that the copper layers partially pulled away from the tungsten layers. The copper layers plastic deformation is observed as the central ridge each formed, while the surface of the tungsten layers is rough and not peaked. While the optical image provides color to help distinguish the layers, the drawbacks are the limited resolution and difficulty with glare on metal samples. In contrast, the SEM gives more detail on the surface structure, but in this case does not give distinct elemental contrast between the tungsten and copper layers (Figure 9). The optical and SEM imaging of the tensile samples will continue so that the modes of failure can be investigated.

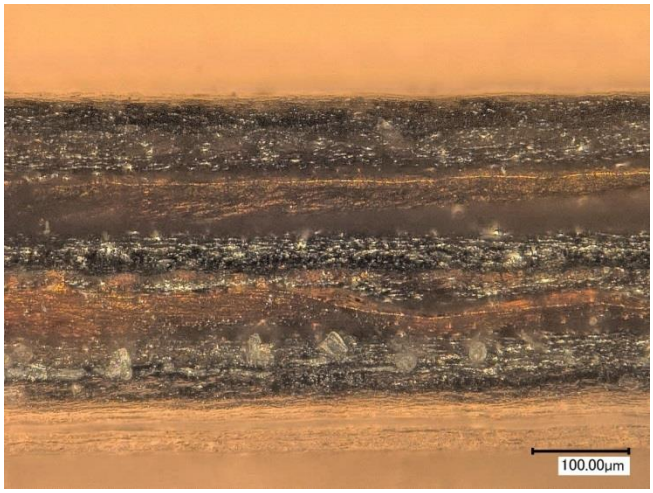

Figure 8. Optical image of fracture surface of SW36 tensile tested at 650°C.

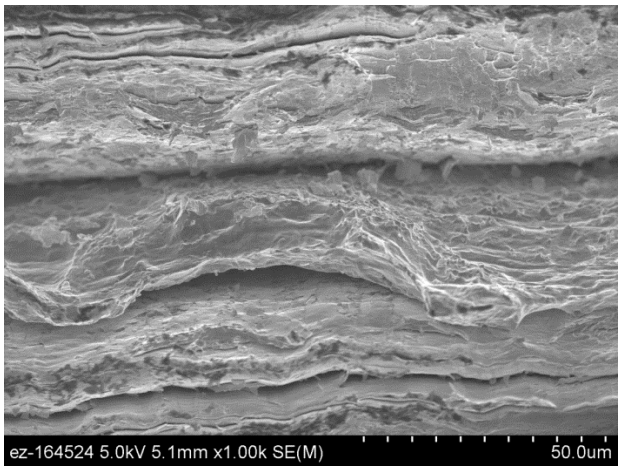

Figure 9. SEM image of unirradiated sample SW37 tested at 500°C.

Important characteristics of a material for fusion applications are its ductility and fracture toughness. Shear punch testing is a well-known technique for characterizing ductility that has several advantages for irradiated tungsten samples. The method uses only small amounts of material, so is suitable for irradiated samples, and is not sensitive to edge machining defects, which is beneficial for a brittle material such as tungsten. Initial investigations have begun with this technique for the copper-tungsten laminate samples.

Microstructure Analysis—Atom Probe

The ORNL-CNMS Cameca Instruments Local Electrode Atom Probe (LEAP) was used to identify and characterize the second phase precipitates formed during the irradiation of single crystal (011), nominally pure tungsten to doses up to 2.2 displacements per atom (dpa) at a temperature of approximately 750 °C.

For the 0.16 dpa irradiated specimen, the recorded time-of-flight spectra indicated that the tungsten had undergone some neutron-induced transmutation, with the primary transmutation products being Os and Re resulting in a bulk composition of W-0.4Os-0.7Re (at.%). The atomic reconstruction of the atom probe data shows the presence of fusiform-shaped Re- and Os-rich clusters (Figure 10a). The average composition of these clusters was found to be W-2.8Os-7.4Re (at.%), with a small spread in compositions, as shown in Figure 10b.

The neutron-induced transmutation in the sample irradiated to 2.2 dpa resulted in a bulk composition of W-7.5Os-5.2Re (at.%). Again, precipitates rich in Os and Re are formed under irradiation, Figure 11a. These precipitates have morphologies that could be broadly classified as rod-like, ribbon-like, rod- and ribbon-like, and clusters. The compositions of these individual precipitates in addition to the bulk and average compositions (W-20.2Os-15.9Re) are shown in Figure 11b. All precipitates, with the exception of 2, lie within the sigma phase composition boundary regardless of the morphology.

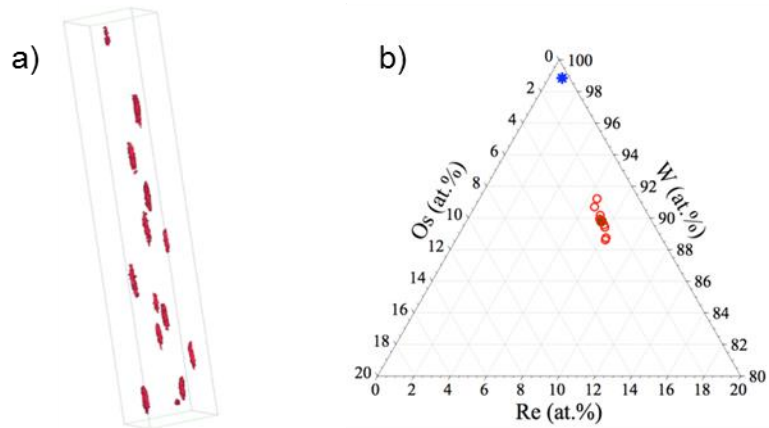

Figure 10. a) Concentration isosurface (ReOs - 20%) from the irradiated tungsten sample. Reconstruction volume is 350 x 60 x 60 nm. b) Ternary diagram showing the composition of individual clusters in the 0.16 dpa irradiated sample. The blue asterisk is the average bulk composition.

There are two points of interest that should be noted regarding the shape and orientation of the precipitates: first, the shape (fusiform, and rod- and ribbon-like) of the neutron irradiated precipitates are vastly different to those formed during self-ion irradiation of a W-1Os-1Re (at.%) alloy in which spherical clusters were formed after irradiations to 33 dpa (1). Second, the precipitates all appear to be crystallographically aligned. Electron backscatter diffraction was used to determine the crystal orientation along the *z*-axis of the atom maps (the long axis of the atom probe needle analyzed). This revealed that the direction of analysis was along the (111) crystal orientation, indicating that there may be some form of preferred diffusion of the solutes along this orientation.

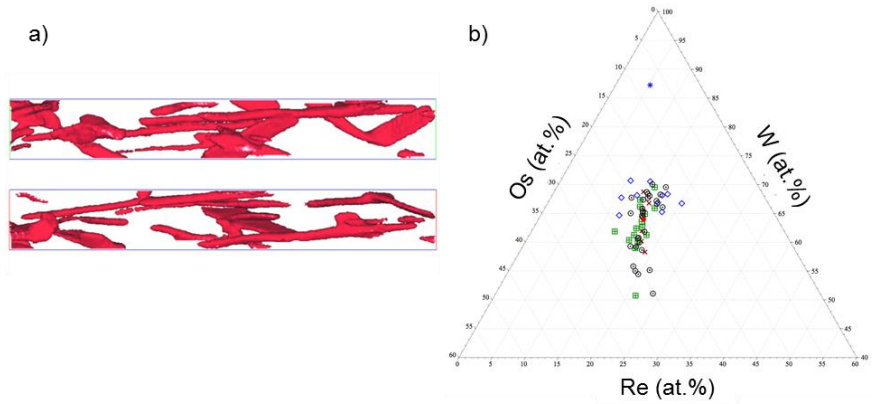

Figure 11. a) Concentration isosurface (ReOs - 20%) from the irradiated tungsten sample. Reconstruction volume is 250 x 35 x 35 nm. b)Ternary diagram showing the composition of individual precipitates (ppt's) found in the irradiated tungsten sample. The blue asterisk is the average bulk composition; red circle is the average ppt composition; the black circles are ribbon-like ppt's; green squares are rod-like ppt's; dark red crosses are rod- and ribbon-like ppt's; and blue diamonds are cluster ppt's.

Microstructure Analysis—TEM

A new set of polycrystalline tungsten specimens exposed to higher neutron doses was selected for further microstructural examination (Table 2). The purpose of selecting these tungsten specimens is to better understand the irradiation-induced transmuted phases and their orientation relation with the tungsten matrix. Selected specimens were mechanically polished in order to remove the oxide layer from the metal surface. A focused ion beam (FIB) system with Ga^+ ion beam was used to prepare TEM specimens. In order to minimized the unwanted damage caused by Ga^+ ions on the TEM specimen, very low energy of 2 kV and 27 pA was used during the final thinning process. The TEM sample preparation and examination is ongoing.

Table 2. Pure tungsten polycrystalline specimens selected for TEM examination.

Sample ID	Target Irradiation Temp (ºC)	Fluence ($x10^{25}$ n/m^2)	dpa	FIB – TEM specimen preparation
OW158	650	7	2.2	Finished
OW125	500	12	3.8	Finished
OW159	650	12	3.8	
AW170	650	12	3.8	
AW134	500	12	3.8	
AW165	650	7	2.2	
OW097	300	7	2.2	
AW098	300	7	2.2	

References

[1] A. Xu *et al*, Acta Mater. **87** (2015) 121